Variations of marine heatwaves and cold spells in the Northwest Atlantic during 1993-2023

Li Zhai[1], Youyu Lu[1], Haiyan Wang[2], Gilles Garric[3], Simon Van Gennip[3]

[1]Fisheries and Oceans Canada, Bedford Institute of Oceanography, 1 Challenger Dr. Dartmouth, NS, B2Y 4A2, Canada
[2]Key Laboratory of Marine Hazards Forecasting, National Marine Environmental Forecasting Center, Ministry of Natural Resources, Beijing, China
[3]Mercator-Ocean International, 2 Av. de l'Aérodrome de Montaudran, 31400 Toulouse, France

Correspondence to: Li Zhai (Li.Zhai@dfo-mpo.gc.ca)

Abstract.

Characteristics of marine heatwaves (MHWs) and cold spells (MCSs) in the Northwest Atlantic during 1993-2023 are derived from a global ocean reanalysis product of the European Union Copernicus Marine Service. For surface parameters, the quantification using the reanalysis data is more advantageous than using the satellite remote sensing data in regions with the presence of seasonal sea ice and strong eddies. At the sea bottom, the reanalysis data well reproduces the observed rising trend and sharp increase of bottom temperature around 2012 on the Scotian Shelf and associated changes of MHW/MCS parameters. The 31 years of reanalysis data enables the quantification of spatial variations, interannual variations and long-term trends of MHW/MCS parameters in the water column in our study region.

The corresponding parameters of surface MHWs and MCSs are overall similar due to the nearly symmetrical probability distribution of sea surface temperature (SST) anomalies around the mean. On the Scotian Shelf, the MHW parameters present layered structures in the water column, influenced by the heat flux in the upper layer and the different water mass compositions in the deeper layer. During 1993-2023, the surface MHW (MCS) total days show increasing (decreasing) trends corresponding to the gradually increasing SST, and the MHW total days reached a peak value of 215 days in 2012 corresponding to the highest annual SST. The bottom temperature shows a stronger increasing trend than the SST, and a regime shift around 2012, resulting in the increasing (decreasing) trend and regime shift of bottom MHW (MCS) total days. In 2012, the bottom MHW total days experienced a sharp increase and the entire water column was warmer than the climatology. The opposite condition presented in 1998 with the longest bottom MCS total days of ~300 near the coast. The quantification of the extreme conditions in 2012 and 1998 supports the results of previous studies on the impacts of these conditions on several marine life species.

1 Introduction

Marine heatwaves (MHWs) and marine cold spells (MCSs) are extreme warm and cold events of the ocean water, respectively. MHWs have been observed in all ocean basins (Collins et al., 2019) and have been extensively studied. Globally, MHWs, defined relative to a fixed climatological period, have become more frequent, long-lasting, and intense since the 1980s under global warming (Frölicher et al., 2018; Oliver et al., 2018; Fox-Kemper et al., 2021). Regionally, local processes, large-scale climate modes, and teleconnections also play important roles in MHW occurrences (Holbrook et al., 2019; Sen Gupta et al., 2020; Capotondi et al., 2024). For example, in the Northwest Pacific, interannual variations of surface MHWs are correlated with various large-scale atmosphere-ocean indices including the El Niño index (Wang et al., 2024). On the shelf seas of the Northwest Atlantic, nearly half of the surface MHWs are initiated by the positive heat flux anomaly into the ocean, and advection and mixing are the primary drivers for the decay of most MHWs (Schlegel et al., 2021b). On the Newfoundland and Labrador Shelf, the summer and fall MHWs in 2023 were impacted by stratification, winds, and advection (Soontiens et al., 2025). Identifying the physical drivers that trigger and maintain the MHWs (MCSs) is important for understanding and predicting the variations of these events and their impacts on marine ecosystems.

Previous studies have revealed the negative impacts of MHWs and MCSs on marine ecosystems. For example, MHWs can cause coral bleaching, destroy kelp forests, and alter the migration patterns of marine species (Santora et al., 2020; Beaudin and Bracco, 2022). MHWs have also affected commercial fisheries in Canadian waters. In the Northeast Pacific, intense and long-lasting heat events, such as "the Blob", led to fisheries collapses (Free et al., 2023). In Atlantic Canada, extreme heat events affect the physiological behaviour of aquaculture Atlantic Salmon, i.e., the increases of heart rates and decreases of motions (Korus, 2024). The declining North Atlantic right whale population was related to the significant warming in the Gulf of Maine and the western Scotian Shelf over the recent decades (Meyer-Gutbrod et al., 2021). The impacts of the extreme cold (warm) event in 1998 (2012) on fishery species have also been studied. In 1998, shortly after the cold Labrador Slope Water replaced the Warm Slope Water, the catches of porbeagle shark and silver hake in the Emerald Basin dramatically declined (Drinkwater et al., 2003). The widespread 2012 warm event in the Northwest Atlantic, with large anomalies throughout the water column and at the sea bottom, had opposite effects on different commercial fisheries. It adversely impacted the snow crab juvenile stages, resulting in a temporary decrease in snow crab abundance on the western Scotian Shelf (Zisserson and Cook, 2017). In the Gulf of Maine, this warm event caused earlier inshore movement of lobsters in the spring, leading to enhanced lobster growth, an extended fishing season, and record landings (Mills et al., 2013).

Compared with MHWs, there have been fewer studies on MCSs. Globally and regionally, the frequency and intensity of surface MCSs show decreasing trends during 1982-2020 associated with the SST increase (Mohamed et al., 2023; Peal et al., 2023; Schlegel et al., 2021b; Wang et al., 2022). Changes in atmospheric forcing, ocean circulation and coastal upwelling can drive local cold events at sea surface (Schlegel et al., 2017) and throughout the water column in shallow coastal bays (Casey et al., 2024).

Studies on surface extreme temperature events commonly use sea surface temperatures (SST) based on satellite remote sensing (e.g., Wang et al., 2022; Peal et al., 2023). Such studies are limited to the upper ocean and ice-free areas, and the analysis results are impacted by the observational noise, and cloud correction and interpolation schemes used to generate various levels of satellite SST products. Subsurface extreme events have been less well studied due to the scarcity of temperature observations below the surface, leading to limited knowledge about whether and how extreme events at depth have changed over the past decades (Collins et al., 2019). Results from high-resolution numerical ocean models, particularly those reanalysis products achieved through data assimilation, have been alternatively used to study the extreme temperature events, both at surface and at bottom (e.g., Amaya et al., 2023a; Wang et al., 2024). The study of Amaya et al. (2023a) revealed stronger and longer MHWs at bottom than at surface in the shelf seas of North America, but it did not quantify the interannual and long-term variations of MHW characteristics.

Motivated by the results of previous studies, in this study we quantify the space-time variations of MHWs and MCSs in the Northwest Atlantic, from surface to water column to bottom, with the ultimate goal to better support fisheries in this region. Our study region (Fig. 1a) can be sub-divided into: (1) Newfoundland and Labrador Shelf (NLS) to the north of Grand Banks; (2) Grand Banks; (3) Gulf of St. Lawrence (GSL), a semi-enclosed sea connecting to the NLS and Scotian Shelf (SS); (4) Scotian Shelf, an open and rugged shelf, adjoining the Gulf of Maine in the southwest and Scotian Slope off the shelf; (5) Gulf of Maine and Bay of Fundy, a tidally energetic semi-enclosed sea; and (6) Scotian Slope. The physical oceanography in the region is quite complex, due to the influences of the strong multi-scale variability of atmospheric forcing, river runoff, tides, sea-ice, the strong ocean circulation of the Gulf Stream, North Atlantic Current and Labrador Current, and the meso-scale eddies, etc. (e.g., Loder et al., 1998; Brickman et al., 2018; Ma et al., 2022). The water masses of NLS and Grand Banks are strongly affected by the southward Labrador Current that transports cold and fresher water and sea-ice. The Scotian Slope water is influenced by the mixture of warm eddies shed from the eastward Gulf Stream/North Atlantic Current and the occasional westward intrusion of the Labrador Current near the tail of Grand Banks. The GSL is influenced by the significant freshwater discharge of rivers including the St. Lawrence River, sea-ice formed locally and transported in from NLS, and inflows from NLS, Grand Banks and Scotian Slope. The SS is influenced by the outflow from the GSL and the intrusion of Scotian Slope water. The Gulf of Maine and Bay of Fundy are influenced by the SS and the Scotian Slope water. Our analysis results will be mainly based on the daily data from an ocean reanalysis product, in comparison with analyses of satellite SST and mooring observations. Main results include 1) characteristics of the spatial distributions of MHW and MCS parameters; 2) the linkages between surface and water column extreme events; and 3) interannual variations and long-term trends, and their relationship with temperature variations and the forcing mechanisms.

2 Datasets and analysis methods

2.1 Datasets

Table 1 lists the datasets analyzed in this study. Product ref. no. 1 is the daily temperature during 1993-2023 from the global ocean eddy-resolving reanalysis with a 1/12° horizontal resolution, referred to as GLORYS12V1, The GLORYS12V1 temperature data remains continuous in ice-covered regions, which helps to compensate for the limitations of spatial and temporal coverage of satellite observations in those areas.

Products ref. no. 2 during 1993-2016 and no. 3 during 2017-2023 are global ocean SST analyses produced daily on an operational basis at the Canadian Meteorological Centre (CMC). The analysis incorporates *in situ* observations and retrievals from one microwave and three infrared sensors (Brasnett, 2008), referred to as CMCSST. According to the assessment by Fiedler et al. (2019), the CMCSST data show low standard deviations and mean differences to the independent Argo observations, in comparison with other long-term SST analyses including the ESA SST CCI (European Space Agency Sea Surface Temperature Climate Change Initiative) and MyOcean OSTIA (Operational Sea Surface Temperature and Ice Analysis) available from the Copernicus marine catalogues. Product ref. no. 3 at 0.1° resolution during 2017-2023 is linearly interpolated onto the 0.2° grids of product ref. no. 2, thus creating a dataset on unified grids covering 1993-2023. CMCSST has no values at locations and time when sea ice is present.

Product ref. no. 4 is the observed daily bottom temperature since 2008 from a bottom-mounted mooring at a location on the inner Scotian Shelf with a water depth of 160 m (Fig. 1, location 1), from the Atlantic Zone Monitoring Program (AZMP) of Fisheries and Oceans Canada. The mooring is situated on the path of the coastal Nova Scotia Current (Hebert et al., 2023). The mooring is redeployed annually in the fall AZMP survey, and the data is only available until September 2023 for this study.

Product Ref. No. & Abbreviation	Product ID & type	Data access	Documentation
1: GLORYS12v1	GLOBAL_MULTIYEAR_PHY_001_030, numerical models	EU Copernicus Marine Service Product (2023) https://doi.org/10.48670/moi-00021	Product User Manual (PUM): Drévillon et al., 2023a Quality Information Document (QUID): Drévillon et al., 2023b Journal article: Lellouche et al., 2021
2: CMCSST	GHRSST Level 4 CMC 0.2 deg global sea surface temperature analysis, 1993-2016	https://doi.org/10.5067/GHCMC-4FM02	Journal article: Brasnett, 2008; CMC 2012
3: CMCSST	GHRSST Level 4 CMC 0.1 deg global sea surface temperature analysis, 2017-2023	https://doi.org/10.5067/GHCMC-4FM03	Journal article: Meissner et al., 2016; CMC 2016
4: mooring data	Mooring bottom temperature at ~ 160 m from the AZMP	https://www.dfo-mpo.gc.ca/science/data-donnees/azmp-pmza/index-eng.html	Hebert et al., 2023

112   **Table 1: Product reference table.**

113

114   **2.2 Definition and quantification of marine heatwaves and cold spells**

115   Following Hobday et al. (2016), the MHWs are defined as periods of extremely warm water that last continuously

116   for five or more days. The MCS are defined similarly as anomalously cold water events following Schlegel et al. (2017).

117   We use the SST data to compute the surface MHW and MCS parameters, and the temperature at ocean floor to compute the

118   bottom MHW and MCS parameters. A seasonally varying climatological percentile threshold method is used to detect

119   MHWs (MCSs). No detrending is applied to the temperature data prior to the MHW/MCS analysis because we want to

120   maintain the consistency and be able to compare with the results of other studies in the Northwest Atlantic (Galbraith et al.,

121   2024; Soontiens et al., 2025), and to emphasize the effects of ocean warming on the changing characteristics of

122   MHWs/MCSs. The climatological mean and thresholds (90th and 10th percentiles of data values) are calculated for each day

123   of the year with all data from multiple years within an 11-day window centred on that day. The climatology and thresholds

124   are defined over 30 years from 1993 to 2022 for GLORYS12V1 and CMCSST, and from 2010 to 2022 for the mooring data.

125   A 30-day 'moving window' is applied to smooth the daily climatology. The MHWs and MCSs are defined for temperatures

126   above the 90th and below the 10th percentile values, respectively. Events that occur less than 2 days apart are considered as

127   one continuous event. The statistics for each MHW (MCS) event are calculated using a Matlab-based tool (Zhao and Marin,

128   2019). This study will focus on the annual statistics of frequency, total days and mean intensity. Frequency refers to the total

129   count of MHW (or MCS) events in each year, while total days are the total number of MHW (or MCS) days in each year.

130   The duration of each MHW (MCS) event is defined as the period over which the temperature is greater (lower) than the

131   seasonally varying threshold value. The intensity of each event is the mean SST anomaly during that event. The mean

132   intensity is the average of the intensities of events during that year.

133   **3 Results**

134   **3.1 Spatial distribution of annual surface MHW and MCS parameters**

135   For surface MHWs, GLORYS12V1 and CMCSST data (Figs. 1c-f) obtain overall similar magnitudes and spatial

136   patterns of mean intensity, but different magnitudes of frequency in deep waters and total days in the seasonally ice-covered

137   areas. For frequency (Figs. 1a and d), both data obtain values of 1-2 events per year on the shelf; and in deep regions (near

138   and beyond the 2000 m isobath) GLORYS12V1 and CMCSST obtain higher and lower than 2.5 events per year,

139   respectively. For the total days (Figs. 1b and e), GLORYS12V1 and CMCSST obtain similar values greater than 30 days per

140   year beyond the shelf break on the Scotian Slope and to the east of the Labrador Shelf, and over the Grand Banks. Over the

141   Newfoundland and Labrador Shelf and in the southern and western Gulf of St. Lawrence where the seasonal sea-ice

142   coverage exists, GLORYS12V1 obtains 25-30 days, higher than about 20 days from CMCSST. In the Gulf of Maine, eastern

143   Scotian Shelf and eastern Gulf of St. Lawrence, GLORYS12V1 obtains 25-30 days while CMCSST obtains 20-25 days. For

144   the mean intensity (Figs. 1c and f), both GLORYS12V1 and CMCSST obtain consistently higher values of 3-6°C in the deep

145   water of the Scotian Slope and to the east of the southern Grand Banks, and lower values of less than 2.5°C on the shelf and

146   in the deep water to the east of the Labrador Shelf. The MHW parameters derived from GLORYS12V1 are consistent with

147   those based on the thermograph network daily mean temperatures in the Gulf of St. Lawrence using the 1991-2020 reference

148   period (Galbraith et al., 2024).

149
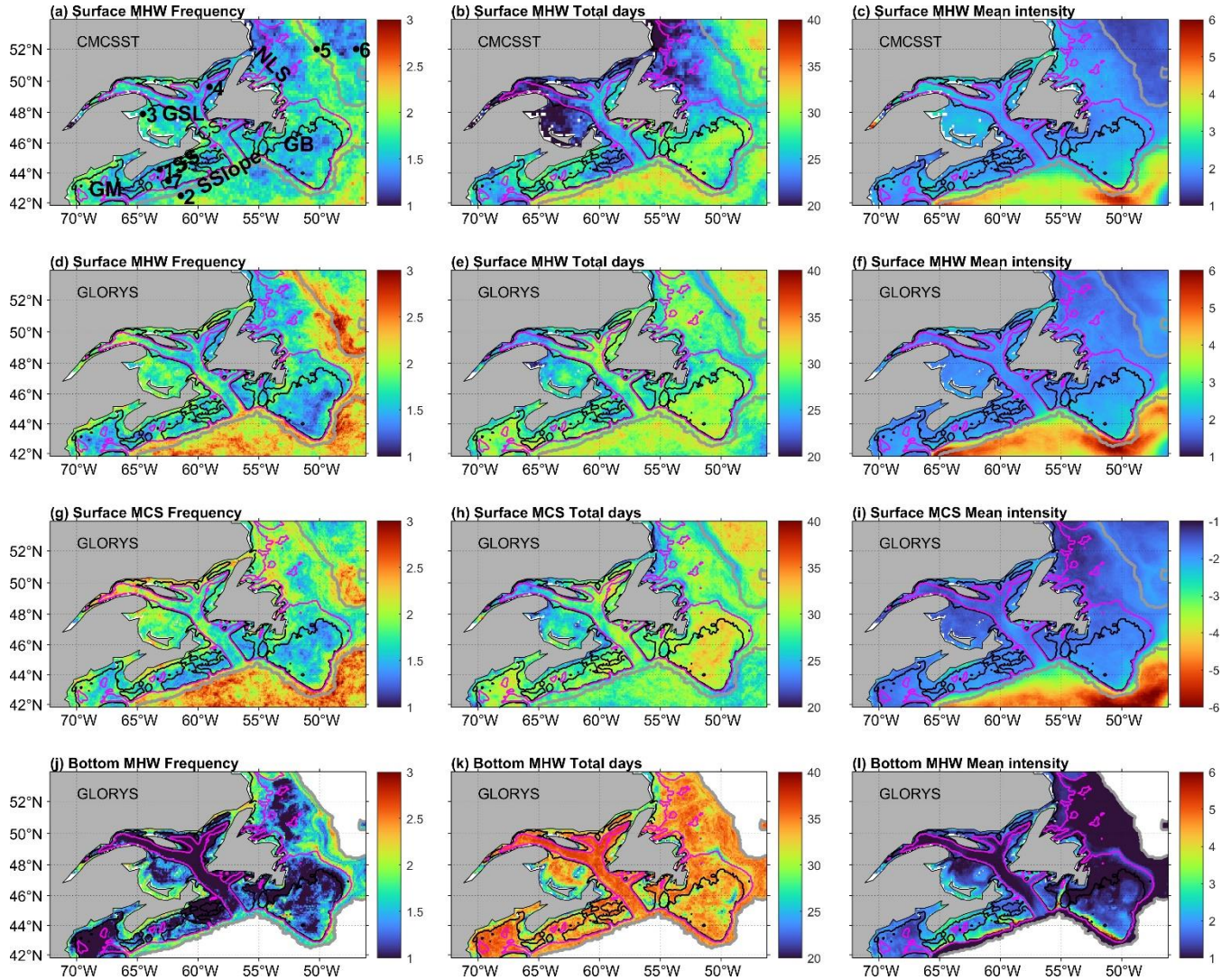
151   **Figure 1: Mean of surface MHW (a-f) and MCS (g-i) characteristics during 1993-2022 derived from (a-c) CMCSST and (d-i)**

152   **GLORYS12V1. (j-l) Mean of bottom MHW characteristics during 1993-2022 derived from GLORYS12V1. From left to right:**

153   **frequency (number of events per year), total days (days per year), and mean intensity (°C). The 100, 200 and 2000 m isobaths are**

154   **represented by black, magenta and grey lines respectively. Panel (a): Stations 1-7 indicated by the solid circles for examining the**

155   **time series of MHW/MCS characteristics, located at latitudes/longitude of 44.25°N/63.16°W, 42.48°N/61.43°W, 47.91°/64.56°W,**

156 **49.64°N/59.06°W, 51.99°N/50.25°W, 52.00°W/47.00°W, and 43.48°N/62.45°W. The Halifax line is the line between stations 1 and 2.**
157 **Abbreviations: GB, Grand Banks; GM, Gulf of Maine; GSL, Gulf of St Lawrence; NLS, Newfoundland and Labrador Shelf; SS,**
158 **Scotian Shelf; SSlope, Scotian Slope; CB, Cabot Strait.**

159

160

The causes of the differences in the MHW parameters derived from GLORYS12V1, CMCSST and mooring data, and the spatial distributions derived from GLORYS12V1, are explored through examining the time series of sea temperatures and the detection of MHWs at selected locations (denoted in Fig. 1a) in selected years, and the variance-preserving spectra during 1993-2022 shown in Fig. 2. The selection of years is based on annual time series of the MHW parameters at these locations (not shown), ensuring that the differences in the MHW parameters between the left and middle columns are consistent with the 1993-2022 averaged statistics shown in Fig. 1. First, on the Scotian Slope the higher surface MHW frequency from GLORYS12V1 than from CMCSST can be explained by their differences in the variance-preserving spectra of the SST time series during 1993-2022 at location 2 (Fig. 2c). Compared with CMCSST, GLORYS12V1 achieves higher spectral power at time scales shorter than 50 days. In the selected year 2023, GLORYS12V1 shows the more frequent and stronger SST variations, and detects three shorter MHW events whereas CMCSST detected one longer MHW event. Note that the high-frequency SST variations in CMCSST are impacted by the cloud correction and interpolation schemes applied to the original satellite data in generating the CMCSST product.

In the southern and western Gulf of St Lawrence, the St. Lawrence Estuary, and on the Labrador and Newfoundland Shelf, CMCSST has shorter total days than GLORYS12V1 (Figs. 1b and e). In the selected year 2011, Fig. 3A presents the SST time series at a location (52.8°N, 55.2°W) on the Labrador Shelf. The original CMCSST data has a significant number of missing values from January to April during the presence of seasonal sea-ice (Fig. A3a), leading to the 90th threshold above that derived from GLORYS12V1 (Figs. A3a and b). If the missing values of the original CMCSST are filled with a freezing temperature of -1.8 °C, the resulting 90th threshold (Fig. A3c) and the total days of the detected MHWs are closer to that derived from GLORYS12V1 (Figs. A3 b). Thus, the shorter MHW total days from CMCSST in regions with the presence of seasonal sea-ice are due the biased 90th threshold caused by the missing SST data values.

The spatial patterns of surface MHW parameters from GLORYS12V1 (Figs. 1d-f) are explained next. The differences between the shelf and the Scotian Slope are demonstrated by comparing the SST time series in 2016 and spectra at locations 1 and 2 (Figs. 2d-f). At all the time scales, location 2 shows much stronger SST variability because it is located in the Scotian Slope where the water mass is affected by a succession of warm and cold oscillations and eddies. In the selected year 2016, GLORYS12V1 detects 6 strong MHW events at location 2 while only one weak event at location 1. In the Gulf of St. Lawrence, the average annual frequency (Fig. 1d) is lower in the northeastern (location 4) and higher in the southwestern (location 3) regions, while the total days (Fig. 1e) show the opposite pattern. This is consistent with the SST time series in the selected year 2012 (Figs. 2g-h), and the variance preserving spectra (Fig. 2i). That is, the spectral energy at location 3 is higher at time scales shorter than 100 days hence leading to higher MHW frequency, and at location 4 is higher at time scales longer than 100 days hence leading to longer durations. The higher total days at station 4 in 2012 are

196 due to the long durations of warming above climatology in fall and winter. Off the Labrador Shelf, over a narrow zone near

197 the 2000 m isobath (location 5), the surface MHW frequency is higher while the total days are shorter, compared to shelf

198 water to the west and the deep water to the east (location 6). This again can be explained by the stronger SST variability at

199 time scales shorter than 100 days at location 5 and longer than 100 days at location 6, respectively (Figs. 2j-l). Location 5 is

200 along the path of the offshore Labrador Current, where the SST anomalies and seasonal cycle are both strong, which can be

201 attributed to the variations of the temperature front in this area (e.g., Lu et al., 2006).

202   For the surface MCSs derived from GLORYS12V1, their frequency, total days and mean intensity (Figs. 1g-i) show

203 similar magnitudes and spatial distribution with those of surface MHWs (Figs. 1d-f). The MCS parameters derived from

204 CMCSST (not shown) is also similar to the surface MHW parameters derived from GLORYS12V1 (Figs. 1a-c). Differences

205 between the MCS and MHW parameters derived from GLORYS12V1 are evident in some areas, e.g., on the Scotian Slope

206 (near location 2) the MHWs have higher mean intensity than the MCSs. These similarities and differences can be explained

207 by the probability distribution of SST anomalies at representative sites shown in Fig. A1. The normalized histograms are

208 nearly symmetrical around the mean, with equal median and mean values. At location 2 the median value is less than the

209 mean, suggesting a positive skewness of SST anomalies on the Scotian Slope due to the dominance of warm-core eddies at

210 the poleward side of the Gulf Stream (e.g., Thompson and Demirov, 2006). Such asymmetric distribution of SST anomalies

211 corresponds to stronger MHWs than MCSs (Schlegel et al., 2021a; Wang et al., 2022).

212

213 **3.2 Distribution of MHW parameters over the sea floor and in the water column**

214   The frequency, total days and mean intensity of bottom MHWs on the shelf derived from GLORYS12V1 (Figs. 1j-

215 l) show different magnitudes and spatial distributions compared to surface MHWs. Our findings are consistent with Amaya

216 et al. (2023a) who showed that bottom MHW intensity and duration vary strongly with bottom depth. The bottom MHW

217 frequency (Fig. 1j) shows fewer events (< 1 per year) in deep basins and channels, and more events (2-3 per year) along the

218 coast and shelf break. The bottom MHW total days (Fig. 1k) exhibit weak spatial variations across the entire region with

219 values of 30-35 days per year, and larger values in deeper basins and channels than in shallow waters. This implies that the

220 bottom MHW durations (roughly total days divided by frequency) are longer in deep basins and channels than in shallow

221 water. The bottom MHWs intensity (Fig. 1l) ranges from 1°C in deeper parts of the continental shelves to 6°C along the

222 edges of the Scotian Shelf and southern Grand Banks where water intrusions from the shelf break occur.

223   We selected two locations on the Scotian Shelf (locations 1 and 7) to illustrate the difference in MCS characteristics

224 at the sea floor (Figs. 2m-o). Location 1 is the mooring site near the coast where the water depth is 160 m, and location 7 is

225 on the Emerald Bank in the middle of the Scotian Shelf where the water depth is 66 m. At location 1, both GLORYS12V1

226 and mooring data (Fig. 2m) show that bottom temperatures in 2016 were generally above the mean climatology and extreme

227 heat events are detected throughout the year. However, mooring data shows some intense cold spikes that are not captured

228 by GLORYS12V1 (Fig. 2m). Correspondingly, compared with the mooring data, the spectral energy of GLORYS12V1 is

229   lower at time scales shorter than 100 days and higher at longer than 100 days (Fig. 2o). At location 7, GLORYS12V1 detects

230   two MHW events with longer durations in 2016 (Fig. 2n). The power spectra (Fig. 2o) show that location 1 has more energy

231   at time scales shorter than 100 days, corresponding to higher MHW frequency and mean intensity, while location 7 shows

232   stronger variability at time scales longer than 100 days, corresponding to longer MHW duration and lower intensity. The

233   strong variations of bottom temperature at shorter than 100 days at location 1 are likely related to the strong fluctuations of

234   the coastal Nova Scotia Current driven by local winds at synoptic scales (Dever et al., 2016).

235

236

237

238

239
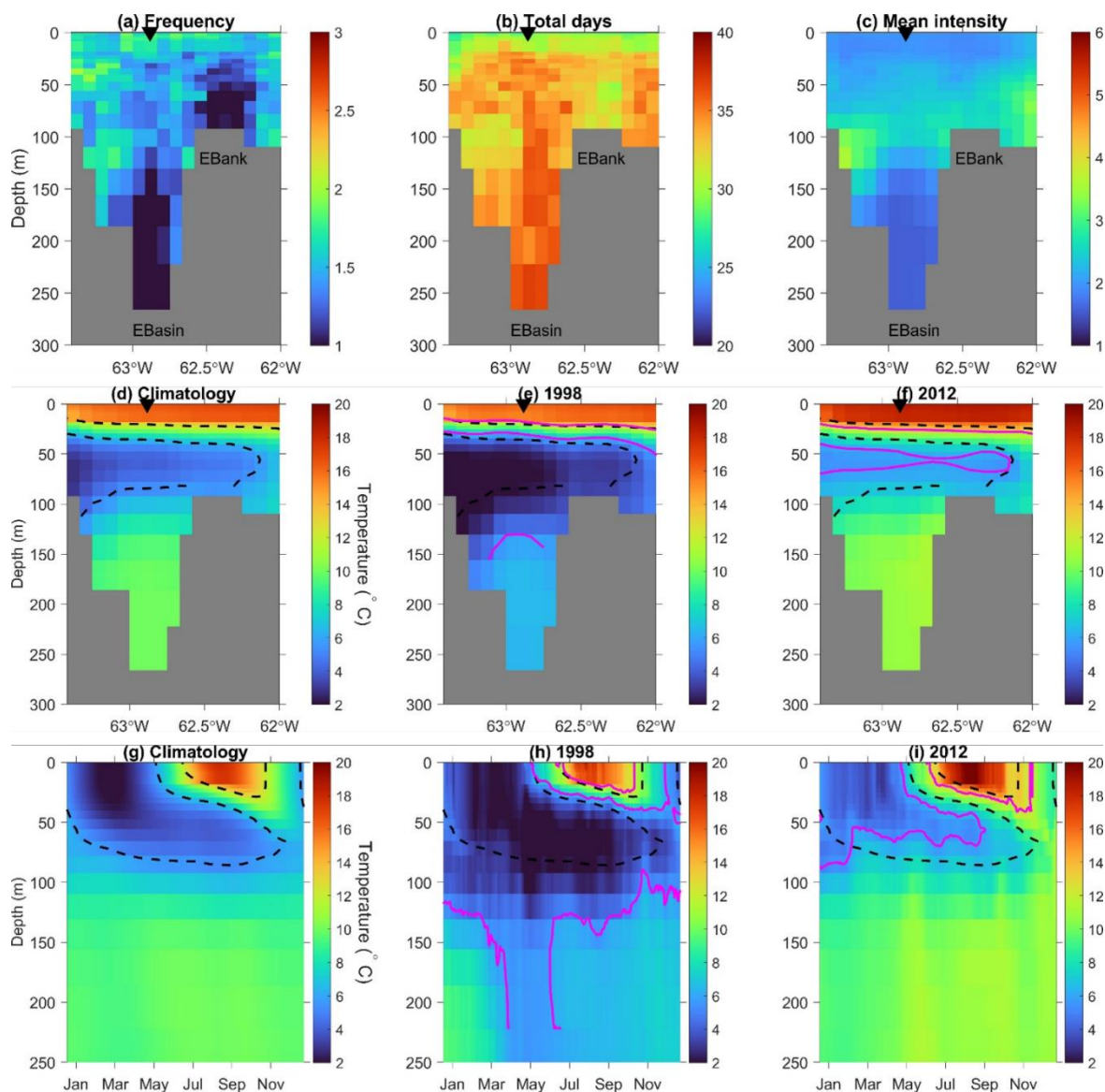
Figure 3: Along the Halifax line (a line between stations 1 and 2 shown in Fig. 1a): MHW (a) mean annual frequency (number of events per year), (b) mean of annual total days (days per year), and (c) mean intensity (°C); summer (July-September) temperature (d) climatology over 1993-2022, in (e) 1998 and (f) 2022. At a station along the Halifax line (marked as the solid black triangle in panels a-f): Seasonal evolution of temperature (g) climatology over 1993-2022, in (h) 1998 and (i) 2012. Contour lines denote the isotherms of 6 and 12 °C: (d-i) dashed black contours for averages over 1993-2022, and solid magenta contours in (e, h) 1998 and (f, i) 2012. Abbreviations: EBasin, Emerald Basin; EBank, Emerald Bank.

To examine the linkages between surface and water column extreme events, we show the distributions of MHW parameters in the water column along the section extending off the coast from Halifax between stations 1 and 2 (Figs. 3a-c). This cross-section, referred to as the Halifax Line, has been regularly occupied by the AZMP over multiple decades thus

251 providing extensive observed hydrographic data to assess the quality of model-based data such as GLORYS12V1. The

252 MHW mean intensity (Fig. 3c) shows a clear 3-layer structure, with values of about 2ºC in the upper layer from surface to a

253 mid-depth interface (decreasing from about 70 m near the coast to about 30 m on the Emerald Bank), high values of 3-3.5ºC

254 in the middle layer from the mid-depth interface to about 130 m, and low values of 1.5-2ºC below 130 m depth in the

255 Emerald Basin. The annual MHW frequency (Fig. 3a) is relatively uniform in the water column with values 1.5-2, except

256 low values (<1) below 130 m depth in the Emerald Basin and below 30 m depth over the Emerald Bank where the annual

257 MHW duration is high.

258 The distribution of MHW parameters in the water column can be explained by the layered structure of temperature

259 along this section in summer (Figs. 3d-f) and the seasonal evolution of the vertical profiles of temperature at a location in the

260 middle of Emerald Basin (Figs. 3g-i), for the mean climatology over 1993-2022, and in the cold and warm years of 1998 and

261 2012, respectively (Hebert et al., 2023). The upper layer (from the surface to 50 m) shows strong seasonal variations. This

262 layer is well mixed in fall/winter, and has strong stratification developed from spring to summer. Seasonal and interannual

263 variations in this upper layer are mainly due to variations of the surface heat flux, and near the coast are also influenced by

264 the outflowing waters from the Gulf of St. Lawrence with strong seasonal and interannual variations in temperature and

265 salinity (Umoh and Thompson, 1994; Dever et al., 2016). The overall major influence of surface heat flux results in a nearly

266 uniform distribution of the MHW parameters in the upper layer. The middle layer (from 50 m to about 130 m depth) presents

267 moderate seasonal variations which can be related to the downward penetration of the surface anomalies driven by surface

268 winds and mixing. On the other hand, this layer is also influenced by the lateral advection of water masses carried by the

269 horizontal currents, mainly from the Cabot Strait subsurface water (30-50 m) and the warm Scotian Slope water and with a

270 smaller portion from the Cabot Strait cold-intermediate layer (50-120 m) and the inshore Labrador Current (Dever et al.,

271 2016). The contributions of the lateral advection vary from the coast to offshore, resulting in the depth range of the mid-

272 depth layer getting smaller from near the coast to the Emerald Bank. The influences of surface forcing and horizontal

273 advection cause high MHW intensity across the whole mid-depth layer, and the low MHW frequency over the Emerald

274 Bank. The deep layer below 130 m depth in the Emerald Basin (Fig. 3g) presents weak seasonal variations with a near

275 constant temperature of 10ºC. However, this layer became colder in 1998 and warmer in 2012 than the climatology (Figs.

276 3h-i), suggesting strong interannual variations of temperatures in this layer. The temperature variations in this deep layer are

277 mainly caused by the intrusion of the offshore water (Dever et al., 2016), leading to low MHW intensity and frequency, and

278 long durations.

279

280 **3.3 Interannual variations of MHW/MCS parameters**

281 Interannual variations of the MHW/MCS parameters at location 1 in the inner Scotian Shelf are presented in Fig. 4,

282 and some of their statistical quantifications are summarized in Table 2. For the surface parameters (Fig. 4 left column),

283 variations of their values derived from GLORYS12V1 have high correlations with those derived from CMCSST except for

284 the MCS mean intensity. The surface MHW (MCS) total days (Figs. 4a and e) show strong interannual variations which

285   have significantly positive (negative) correlations with the annual SST anomalies from GLORYS12V1 (Table 2). The

286   MHW/MCS mean intensities show weaker interannual variations and have no significant correlations with the SST

287   anomalies.

288   For the bottom parameters (Fig. 4 right column), significant correlation values derived from GLORYS12V1 and

289   available mooring data are found for the MHW frequency, total days and mean intensity, but not for the MCS parameters

290   (Table 2). This can be attributed to GLORYS12V1 not being able to reproduce the intense cold spikes in the mooring data

291   (Fig. 2m). For both the bottom MHWs and MCSs, interannual variations of their frequency, total days and mean intensity all

292   have significant correlations with the annual bottom temperature anomalies from GLORYS12V1. The bottom MHW total

293   days and mean intensity derived from the mooring data are significantly lower than those derived from GLORYS12V1. This

294   is due to the differences in the bottom temperature climatology of the two datasets defined for the calculation of the

295   MHW/MCS parameters. While the two datasets show similar values and increasing trends in the bottom temperatures, the

296   climatology of mooring data during the 16 years of 2008-2023 has a higher averaged temperature than that of

297   GLORYS12V1 during 30 years of 1993-2022 (Fig. 4j). As a result, the mooring data obtains shorter and weaker bottom

298   MHW events than GLORYS12V1. If the same reference period of 2008-2023 is used, the difference in MHW parameters

299   between mooring data and GLORYS12V1 is largely reduced. This suggests that the calculation of MHW/MCS parameters is

300   strongly impacted by the duration chosen for computing the climatology, and whether detrending is applied, as discussed in

301   Capotondi et al. (2024) and Smith et al. (2025).

302   At location 1 during 1993-2023, both at surface and bottom, interannual variations of the MHW and MCS total days

303   are negatively correlated; the intensity and total days of MHWs show positive trends, while those for MCSs show negative

304   trends (Table 2). These correspond to warming trends in both the SST and bottom temperature (Figs. 4i-j). The MHW and

305   MCS mean intensities show no significant trends at surface, but positive trends at bottom (Table 2). For the bottom

306   MHW/MCS total days, the trends are mostly due to their sharp increases (or regime shift) around 2012 (Figs. 4b and f). Out

307   of the 19 years before 2012, bottom MCS events are detected in 11 years while MHW events are detected only in 2 years. By

308   comparison, out of the 12 years since 2012, bottom MHW events are detected in 10 years while MCS events are detected

309   only in one year. These correspond to the sharp increase of bottom temperature that also occurred around 2012 (Fig. 4j). By

310   comparison, the SST at location 1 shows a more gradual increasing trend (Fig. 4i). After 2012, the annual bottom

311   temperature became higher than the annual SST. As a result, the bottom MHW total days frequently exceed 150, higher than

312   50-100 for large values of the surface MHW total days (Figs. 4a and b). The long-term trends and regime shifts of bottom

313   MHW/MCS total days are widespread on the Scotian Shelf, as evidenced by the similar time series as location 1 at a location

314   in the Emerald Basin and location 7 on the Emerald Shelf (Fig. A2). This raises the question about how to define

315   MHWs/MCSs in the presence of long-term trends or regime changes in ocean temperature, a point to be discussed in Section

316   4.

317   The time series plots identify years when severe MHW or MCS events occurred. At location 1, the surface MHW

318   total days show the highest values in 2012, reaching 215 days according to GLORYS (Fig. 4a). Both GLORYS12V1 and

CMCSST detect 7 MHW events with the duration ranging from 7 to 61 days. These prolonged surface MHW events correspond to the highest peak of annual SST (Fig. 4i) and the well-known warming condition across the Scotian Shelf (Hebert et al., 2013), in the Gulf of Maine and east coast of the USA in 2012 (Chen et al., 2015). In December 2011, the SST in the region was close to the 90th percentile and likely played a role in preconditioning the MHW in January 2012. Chen et al. (2015) further attributed the widespread MHW events to persistent atmospheric high-pressure systems featured by anomalously weak wind speeds, increased insulation, and reduced ocean heat losses. At location 1, the termination of a long-lasting and strong surface MHW event in the summer of 2012 (Fig. 3i) can be attributed to wind-induced coastal upwelling, resulting in a sudden drop in SST at the end of August (Shan and Sheng, 2022).

In 2012 at location 1, the bottom MHW total days experienced a sharp increase relative to previous years, reaching ~100 days according to GLORYS12V1 (Fig.4b). In the summer of 2012, the entire water column along the Halifax Line was warmer than the climatology (Figs. 3d and f). In the Emerald Basin (Figs. 3g and i), the abnormally warm condition presented from the surface to about 100 m depth at the beginning of the year (winter), which can be attributed to the smaller heat loss to the atmosphere at the sea surface. Below the 100 m depth, warming started in spring. Below the upper layer directly influenced by surface forcing, the warming in 2012 can be attributed to advection over the Scotian Shelf between 30-50 m, the advection of anomalously warm slope water combined with the reduced contribution of the cold water from the Gulf of St Lawrence or the inner Labrador Shelf between 50-100m, and the anomalously warm slope water being advected onto the shelf between 100-200 m. (Dever et al., 2016). The warm Scotian Slope water was influenced by the interaction between the Gulf Stream and the Labrador Current at the tail of the Grand Banks (Brickman et al., 2018; Gonçalves Neto et al., 2023).

The condition in 1998 is opposite to that in 2012, i.e., 1) location 1 experienced the longest bottom MCS total days (nearly 300 days) associated with the lowest annual bottom temperature value (Figs. 4f and j); 2) in summer the entire water column along the Halifax Line was colder than the climatology (Figs. 3d and e); and 3) in the Emerald Basin (Figs. 3g and h) the entire water column was anomalously cold throughout the year except for close to normal condition in the upper layer in summer. Below 150 m depth in the Emerald Basin, the lowest temperature occurred during March-June. This can be related to the intrusion of the cold Labrador Slope water. According to Drinkwater et al. (2003), this cold water mass was advected along the shelf break in 1997-1998 and flooded the lower layers of the central and southwestern regions of the Scotian Shelf.

In 2023 at location 1, according to GLORYS12V1, the surface MHW total days is 85 (Fig. 4a), which is well above the average value of 31 days. The mean intensity is 2°C (Fig. 4c), similar to the multi-year averaged intensity. The longest surface MHW event of that year began on December 19, 2022, and continued until February 8, 2023, coinciding with the warmest January on record in Halifax. The termination of this MHW event is likely related to an extremely cold Arctic air outbreak that set many local meteorological records in early February in Atlantic Canada and caused rapid drops of water temperature in some shallow coastal bays (Casey et al., 2024).
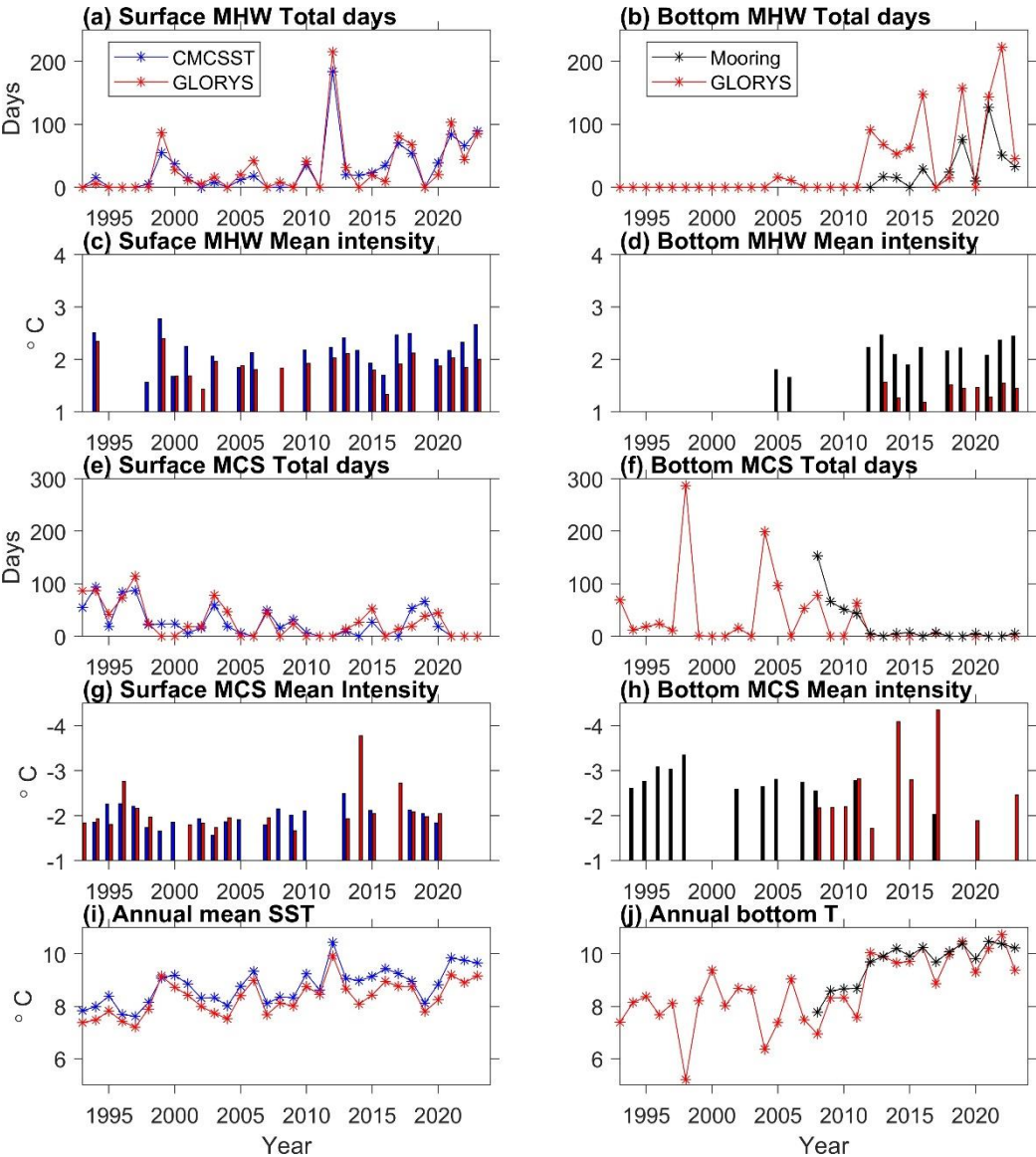
Figure 4: Time series of MHW and MCS characteristics at location 1 (marked in Fig. 1) for surface (a, c, e, g and i) and for bottom (b, d, f, h and j). (a, b) MHW total day; (c, d) MHW mean intensity; (e, f) MCS total days; (g, h) MCS intensity; (i, j) comparison of annual mean time series of GLORYS12V1 with CMCSST and mooring data.

	Trend	Correlation between MHW/MCS from GLORYS12V1 and observations	Correlation between MHW/MCS parameters and T
Surface			
MHW frequency	0.07 events/yr	0.83	0.85
MHW total days	1.9 days/yr	0.96	0.81
MHW intensity	-	0.77	-
MCS frequency	-0.1 events/yr	0.69	-0.80
MCS total days	-1.8 days/yr	0.84	-0.81
MCS intensity	-	-	-
Bottom			
MHW frequency	0.2 events/yr	0.70	0.72
MHW total days	4.1 days/yr	0.69	0.70
MHW intensity	0.03 °C/yr	0.64	0.59
MCS frequency	-0.1 events/yr	-	-0.75
MCS total days	-2.3 days/yr	0.78	-0.78
MCS intensity	0.03 °C/yr	-	0.59

Table 2: Statistics of annual values of MHW/MCS parameters during 1993-2023 at location 1 on the inner Scotian Shelf. Column 2: linear trends of MHW/MCS frequency in events/year, total days in days/year, and mean intensity in °C/year derived from GLORYS12V1. Column 3: correlation coefficient of MHW/MCS parameters derived from GLORYS12V1 and from CMCSST at the surface and mooring temperature at the sea floor. Column 4: correlation coefficient between MHW/MCS parameters and annual GLORYS12V1 temperature. Significant trends and correlations with p-values less than 0.1 are shown.

4 Conclusions and discussions

First, in this study the annual mean MHW/MCS parameters derived from GLORYS12V1 and observational data are compared. At the surface, GLORYS12v1 and CMCSST obtain similar magnitudes, spatial distribution and interannual variations of MHW/MCS frequency, total days and mean intensity. Differences in the values of the parameters can be attributed to issues in the CMCSST data: 1) shorter MHW total days in the Gulf of St. Lawrence and Labrador and Newfoundland Shelf due to the higher threshold values caused by the missing SST data in the presence of ice, and 2) less frequent MHWs on the deep Scotian Slope associated with weaker SST variations caused by the interpolations and cloud correction applied to the satellite remote sensing data for generating the CMCSST. Thus, we suggest that high-resolution data assimilative ocean reanalysis products present more advantages in quantifying surface MHWs and MCSs than SST products based on satellite remote sensing. For the bottom MHWs and MCSs, the analysis results from GLORYS12V1 are

compared with those from 16 years of bottom mooring observations at location 1 near the coast of Nova Scotia. GLORYS12V1 captures all parameters of observed bottom MHWs and the total days of bottom MCSs at this location. However GLORYS12V1 does not reproduce the intense cold spikes of observed bottom temperature and hence detects fewer and less intense bottom MCSs at this location. This can be attributed to the spatial resolution GLORYS12V1 that is insufficient to resolve the sharp spatial gradients of the Nova Scotia Current. Therefore near the coast of Nova Scotia, GLORYS12V1 underestimates the frequency and intensity of the bottom MCSs, although provides estimates of the total days in agreement with the mooring data.

Second, the horizontal/depth distributions of the annual MHW/MCS parameters are explained by the characteristics of temperature variations and the related ocean dynamics. The corresponding parameters of surface MHWs and MCSs are overall similar due to the nearly symmetrical probability distribution of SST anomalies around the mean, except on the Scotian Slope where the MHWs have lower frequency and higher mean intensity than the MCSs due to the dominance of warm-core eddies. The surface MHWs have the highest frequency (2-3 events per year) and mean intensity (3-6°C) on the Scotian Slope and to the east of southern Grand Banks, due to the strong SST variability associated with the eddy activities and variations of Gulf Stream and North Atlantic Current. The shelf waters show nearly uniform values of the surface MHW parameters: 1-2 events per year for frequency, 20-30 days per year for total days, and ~2.0°C for the mean intensity. The bottom MHW frequency, duration (approximately total days divided by frequency) and mean intensity vary strongly with bottom depth, which can be explained by the layered structure of MHW parameters and temperature along a cross-shelf section off Halifax (Fig. 3). In the upper layer from surface to a mid-depth interface, the nearly uniform MHW mean intensity of ~2°C can be mainly attributed to variations of the surface heat flux. From the mid-depth interface to about 130 m depth, the MHW mean intensity has high values of 3-3.5°C which can be related to the combined effects of downward penetration of the upper layer (through wind forcing and mixing) and the lateral advection of water masses from the Cabot Strait subsurface and cold-intermediate layers, the Scotian Slope water and the inshore Labrador Current. In the deep Emerald Basin below 130 m depth, the MHW intensity has the lowest values of 1.5-2°C due to intrusions of offshore water. The MHW frequency has relatively uniform values of 1.5-2 events per year in the water column, except low values of less than 1 event per year (corresponding to longer MHW durations) below 130 m depth in the Emerald Basin and below 30 m depth over the Emerald Bank. This can be attributed to the different characteristics of temperature variations caused by different forcings: stronger variations at shorter (longer) time scales by surfacing forcing (lateral intrusion).

Thirdly, analysis of the GLORYS12V1 data reveals interannual variations, long-term trends and regime shifts of MHW/MCS parameters during 1993-2023. For the surface MHW (MCS) total days, 1) their annual values have significantly positive (negative) correlations with the annual SST anomalies; 2) their increasing (decreasing) trends correspond to the gradual increasing SST; and 3) the peak value (215 days) of MHW total days in 2012 corresponds to the highest annual SST representing the well-known warming condition across the Scotian Shelf, Gulf of Maine and the east coast of the USA. The bottom temperature shows a stronger increasing trend than the SST, and a sharp increase (regime shift) around 2012. This causes the increasing (decreasing) trend and regime shift of MHW (MCS) total days. After 2012 at location 1, the annual

bottom temperature became higher than the annual SST; and the bottom MHW total days frequently exceeded 200, higher than 50-70 for large values of the surface MHW total days. At location 1 near the coast of Nova Scotia, GLORYS12V1 well reproduces the rising trend and sharp increase of bottom temperature around 2012 in the mooring data. In 2012, the bottom MHW total days at location 1 experienced a sharp increase to ~100 days. Consistent with the AZMP observations, GLORYS12V1 shows that in 2012 the entire water column along the Halifax Line was warmer than the climatology, which can be attributed to the smaller heat loss to the atmosphere at the sea surface, the advection of abnormally warm Scotian Slope water, and the reduced contribution of the cold water from the Gulf of St Lawrence or the inner Labrador Shelf. Opposite conditions occurred in 1998 with the longest bottom MCS total days of ~300 days at location 1, and the entire water column along the Halifax Line was colder than the climatology. Further studies are needed to link variations of ocean temperature and MHW/MCS parameters in the Northwest Atlantic, at interannual and longer time scales, to large-scale ocean-atmosphere processes. For example, using long time series of synthetic data, Gregory et al. (2024) recently examined connections between El Niño-Southern Oscillations and variations of MHWs globally, and identified a linkage between La Niña events in the equatorial Pacific and warm conditions in the Northwest Atlantic. Further studies along this line are important for developing predictions of MHWs and MCSs in the future.

We note that the detection of MHWs and MCSs and the quantification of their parameters depend on the reference climatology of ocean temperature, particularly in our study region with evident warming trends over the past several decades. Defining the climatology over 30 years (1993-2022) with the GLORYS data obtains longer total days and stronger intensity for bottom MHWs, compared with using the recent 16 years (2008-2023) of bottom temperature from mooring observations. There are ongoing debates in the literature about whether the long-term trends in ocean temperature should be included or excluded in MHW research (Oliver et al., 2021; Zhang et al., 2024). Recent studies (Amaya et al., 2023b; Capotondi et al., 2024; Smith et al., 2025) suggested that both approaches could be useful depending on the applications of interest. The long-term warming trends and short-duration extreme events likely cause different physiological and behavioural responses of marine species. In the present study, the long-term warming trend is retained in defining the water temperature climatology and the detection of MHWs and MCSs, while in the future we may explore other definitions when investigating the impacts of MHWs and MCSs on marine ecosystems and fisheries.

Data and code availability

The data used in this study are available as described in Table 1. The code used in this study can be accessed via a GitLab repository upon request via email to the corresponding author.

Author contribution

LZ and YL led the conceptualization of the study, analysis and writing of the manuscript. HW refined the scripts of data analysis. GG and SVG contributed to the conceptualization of the study, and editing and reviewing the manuscript.

446

Competing interests

The authors declare that they have no conflict of interest.

Disclaimer

The Copernicus Marine Service offering is regularly updated to ensure it remains at the forefront of user requirements. In this process, some products may undergo replacement or renaming, leading to the removal of certain product IDs from our catalogue. If you have any questions or require assistance regarding these modifications, please feel free to reach out to our user support team for further guidance. They will be able to provide you with the necessary information to address your concerns and find suitable alternatives, maintaining our commitment to delivering top-quality services.

Publisher's note: Copernicus Publications remains neutral with regard to jurisdictional claims in published maps and institutional affiliations.

Acknowledgments

We appreciate DFO and Mercator-Ocean International for supporting the scientific exchanges and collaboration between the staff of both organizations, in recent years under a collaborative agreement, Dr. David Brickman for commenting on an early version of the manuscript, Dr. Karina Von Schuckmann for insightful comments and advice in developing this manuscript, Drs. Xianmin Hu, Justine Mcmillan and Nancy Soontiens for internal reviews, and Dr. Peter Galbraith and two anonymous reviewers for detailed, insightful and constructive comments that helped to improve the original manuscript.

473 **Appendix:**
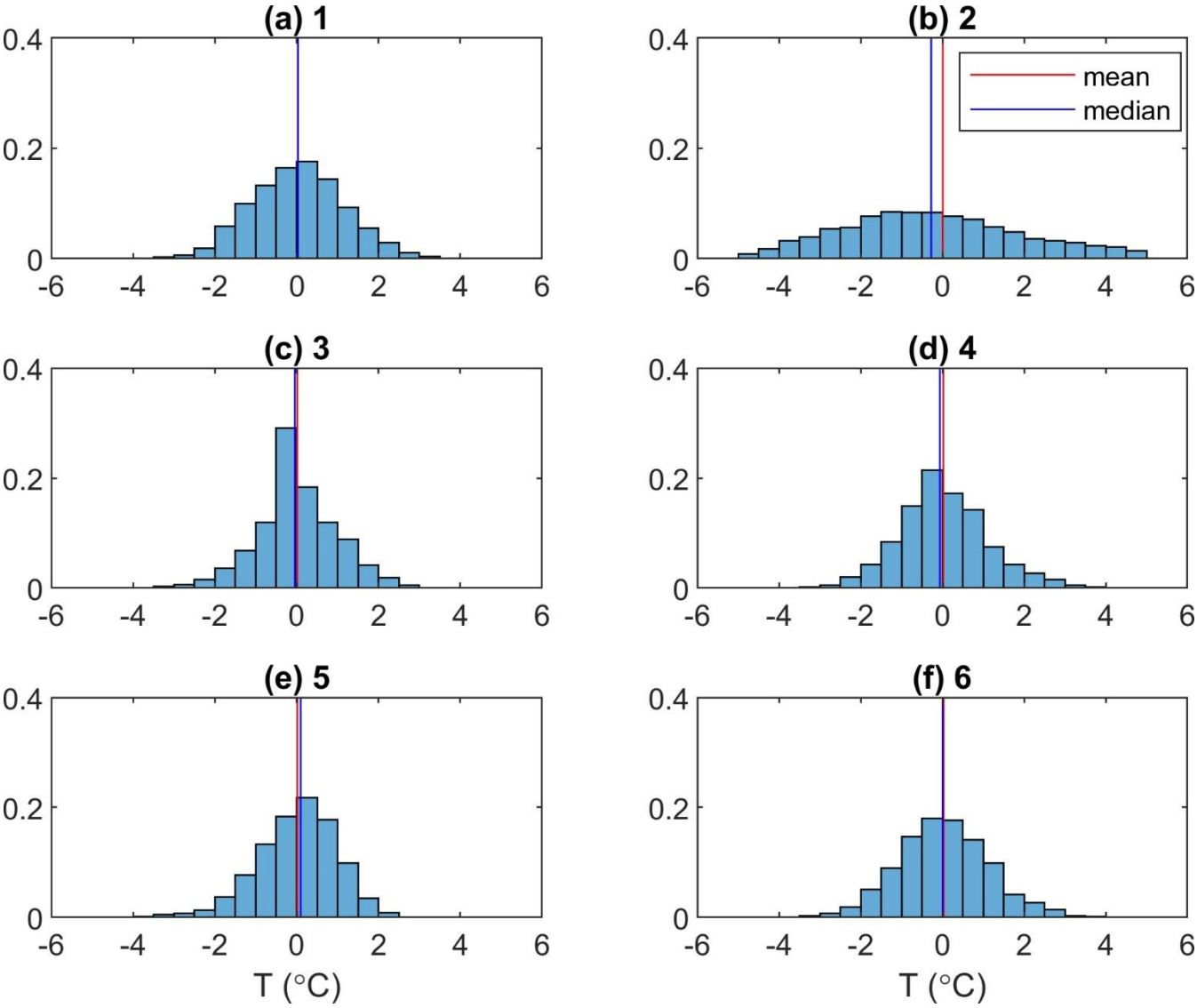
Figure A1: Histogram of sea surface temperature anomalies from GLORYS12V1 at six locations marked in Fig. 1. The height of
each bar is the number of data values in each bin divided by the total number of data values.

478
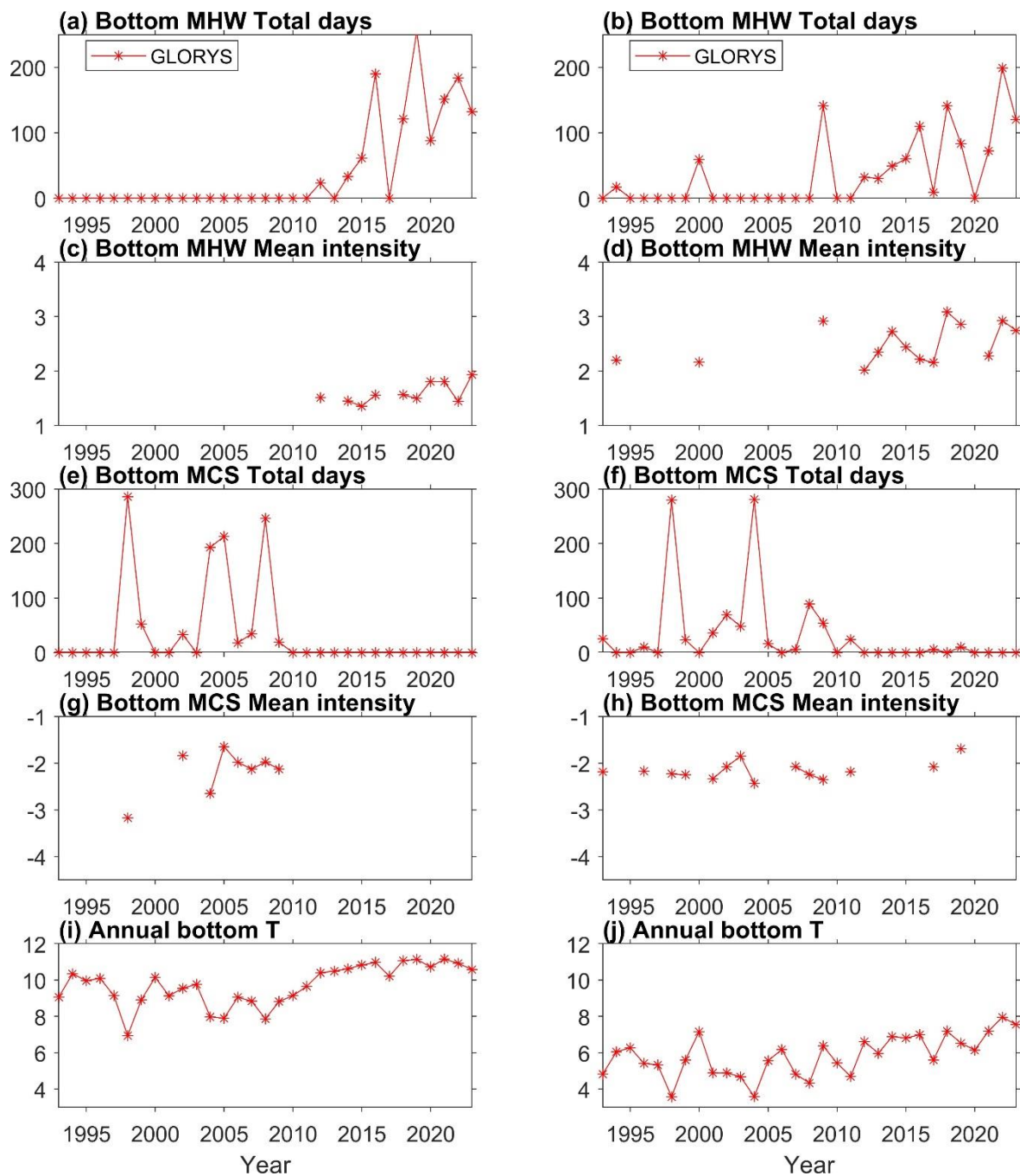
479 **Figure A2. Time series of bottom MHW/MCS parameters and bottom temperature derived from GLORYS12V1 at**

480 **(left column) a location in Emerald Basin (marked as a triangle in Fig. 3a) and (right column) location 7 on Emerald**

481 **Bank (marked in Figure 1a).**

482
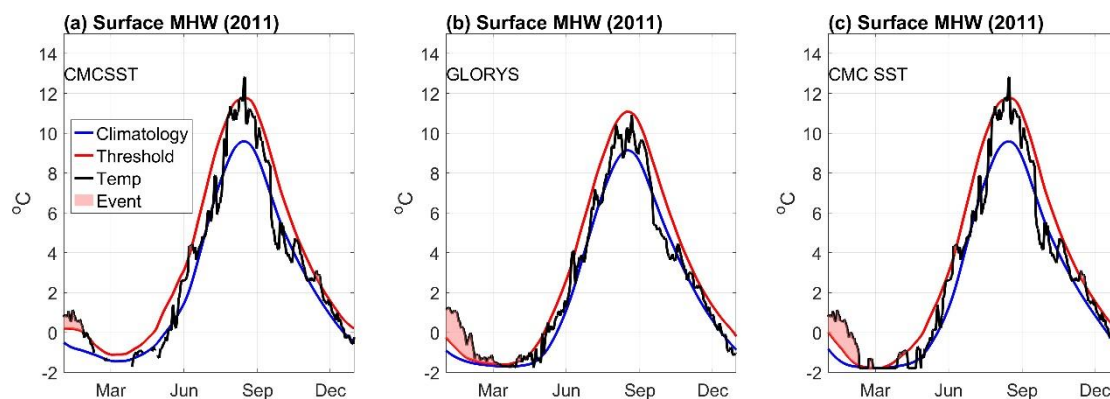
483 **Figure A3. Evolution of surface MHWs in 2011 at a location (52.8°N, 55.2°W) on the Labrador Shelf derived from (a,**

484 **c) CMCSST and (b) GLORYS12V1. In (c) the missing values of CMCSST are filled with the freezing temperature of**

485 **-1.8 °C.**

References:

Amaya, D. J., Jacox, M. G., Alexander, M. A., Scott, J. D., Deser, C., Capotondi, A., and Phillips, A. S.: Bottom marine heatwaves along the continental shelves of North America, Nat Commun, 14, 1038, https://doi.org/10.1038/s41467-023-36567-0, 2023a.

Amaya, D. J., Jacox, M. G., Fewings, M. R., Saba, V. S., Stuecker, M. F., Rykaczewski, R. R., Ross, A. C., Stock, C. A., Capotondi, A., Petrik, C. M., Bograd, S. J., Alexander, M. A., Cheng, W., Hermann, A. J., Kearney, K. A., and Powell, B. S.: Marine heatwaves need clear definitions so coastal communities can adapt, Nature, 616, 29–32, https://doi.org/10.1038/d41586-023-00924-2, 2023b.

Beaudin, É., and Bracco, A.: How Marine Heatwaves Impact Life in the Ocean. Front. Young Minds 10:712528. doi: 10.3389/frym.2022.712528, 2022.

Brasnett, B.: The impact of satellite retrievals in a global sea‐surface‐temperature analysis, Quart J Royal Meteoro Soc, 134, 1745–1760, https://doi.org/10.1002/qj.319, 2008.

Brickman, D., Hebert, D., and Wang, Z.: Mechanism for the recent ocean warming events on the Scotian Shelf of eastern Canada, Continental Shelf Research, 156, 11–22, https://doi.org/10.1016/j.csr.2018.01.001, 2018.

Canada Meteorological Center: CMC 0.2 deg global sea surface temperature analysis. Ver. 2.0. PO.DAAC, CA, USA. Dataset accessed [2023-11-27] at https://doi.org/10.5067/GHCMC-4FM02, 2012.

Canada Meteorological Center: GHRSST Level 4 CMC 0.1 deg global sea surface temperature analysis. Ver. 3.0. PO.DAAC, CA, USA. Dataset accessed [2024-03-05] at https://doi.org/10.5067/GHCMC-4FM03, 2016.

Capotondi, A., Rodrigues, R.R., Sen Gupta, A., Benthuysen, J.A., Deser, C., Frölicher, T.L., Lovenduski, N.S., Amaya, D.J., Le Grix, N., Xu, T., Hermes, J., Holbrook, N.J., Martinez‐Villalobos, C., Masina, S., Roxy, M.K., Schaeffer, A., Schlegel, R.W., Smith, K.E., Wang, C.: A global overview of marine heatwaves in a changing climate. Commun. Earth Environ. 5, 1–17. https://doi.org/10.1038/s43247-024-01806-9, 2024.

Casey, M.P., Petrie, B., Lu, Y., MacDermid, S., and Paquin, JP: Rapid drops of ocean temperatures in several shallow bays in Nova Scotia during a recent cold air outbreak, Proceedings of the Nova Scotian Institute of Science, Volume 53, Part 2, pp. 219-248, 2024.

Chen, K., Gawarkiewicz, G., Kwon, Y., and Zhang, W. G.: The role of atmospheric forcing versus ocean advection during the extreme warming of the Northeast U.S. continental shelf in 2012, JGR Oceans, 120, 4324–4339, https://doi.org/10.1002/2014JC010547, 2015.

Collins M., M. Sutherland, L. Bouwer, S.-M. Cheong, T. Frölicher, H. Jacot Des Combes, M. Koll Roxy, I. Losada, K. McInnes, B. Ratter, E. Rivera-Arriaga, R.D. Susanto, D. Swingedouw, and L. Tibig: Extremes, Abrupt Changes and Managing Risk., in: IPCC Special Report on the Ocean and Cryosphere in a Changing Climate, edited by: H.-O. Pörtner, D.C. Roberts, V. Masson-Delmotte, P. Zhai, M. Tignor, E. Poloczanska, K. Mintenbeck, A. Alegría, M. Nicolai, A. Okem, J. Petzold, B. Rama, and N.M. Weyer, Cambridge University Press, Cambridge, UK and New York, NY, USA, 589–655, https://doi.org/10.1017/9781009157964.003, 2019.

Dever, M., Hebert, D., Greenan, B. J. W., Sheng, J., and Smith, P. C.: Hydrography and Coastal Circulation along the Halifax Line and the Connections with the Gulf of St. Lawrence, Atmosphere-Ocean, 54, 199–217, https://doi.org/10.1080/07055900.2016.1189397, 2016.

Drévillon, M., Fernandez, E., Lellouche, J.M.: EU Copernicus Marine Service Product User Manual for the Global Ocean Physics Reanalysis, GLOBAL_MULTIYEAR_PHY_001_030, Issue 1.5, Mercator Ocean International, https://catalogue.marine.copernicus.eu/documents/PUM/CMEMS-GLO-PUM-001-030.pdf, last access: 19 March 2024, 2023a

Drévillon, M., Lellouche, J.M., Régnier, C., Garric, G., Bricaud, C., Hernandez, O., and Bourdallé-Badie, R.: EU Copernicus Marine Service Quality Information Document for the Global Ocean Physics Reanalysis, GLOBAL_MULTIYEAR_PHY_001_030, Issue 1.6, Mercator Ocean International, https://catalogue.marine.copernicus.eu/documents/QUID/CMEMS-GLO-QUID-001-030.pdf, last access: 19 March 2024, 2023b

Drinkwater, K. F., Petrie, B., and Smith, P. C.: Climate variability on the Scotian Shelf during the 1990s, ICES MSS Vol.219 - Hydrobiological variability in the ICES Area, 1990-1999, https://doi.org/10.17895/ices.pub.19271735.v1, 2003.

Fiedler, E. K., McLaren, A., Banzon, V., Brasnett, B., Ishizaki, S., Kennedy, J., Rayner, N., Roberts‐Jones, J., Corlett, G., Merchant, C. J., and Donlon, C.: Intercomparison of long-term sea surface temperature analyses using the GHRSST

536   Multi-Product Ensemble (GMPE) system, Remote Sensing of Environment, 222, 18–33,
537   https://doi.org/10.1016/j.rse.2018.12.015, 2019.

538 Fox-Kemper, B., Hewitt, H. T., Xiao, C., Aðalgeirsdóttir, G., Drijfhout, S. S., Edwards, T. L., Golledge, N. R., Hemer, M.,
539   Kopp, R. E., Krinner, G., Mix, A., Notz, D., Nowicki, S., Nurhati, I. S., Ruiz, L., Sallée, J.-B., Slangen, A. B. A.,
540   and Yu, Y.: Ocean, Cryosphere and Sea Level Change, edited by: Masson-Delmotte, V., Zhai, P., Pirani, A.,
541   Connors, S. L., Péan, C., Berger, S., Caud, N., Chen, Y., Goldfarb, L., Gomis, M. I., Huang, M., Leitzell, K.,
542   Lonnoy, E., Matthews, J. B. R., Maycock, T. K., Waterfield, T., Yelekçi, O., Yu, R., and Zhou, B., Climate Change
543   2021: The Physical Science Basis. Contribution of Working Group I to the Sixth Assessment Report of the
544   Intergovernmental Panel on Climate Change, 1211–1362, https://doi.org/10.1017/9781009157896.011, 2021.

545 Free, C. M., Anderson, S. C., Hellmers, E. A., Muhling, B. A., Navarro, M. O., Richerson, K., Rogers, L. A., Satterthwaite,
546   W. H., Thompson, A. R., Burt, J. M., Gaines, S. D., Marshall, K. N., White, J. W., and Bellquist, L. F.: Impact of
547   the 2014–2016 marine heatwave on US and Canada West Coast fisheries: Surprises and lessons from key case
548   studies, Fish and Fisheries, 24, 652–674, https://doi.org/10.1111/faf.12753, 2023.

549 Frölicher, T. L., Fischer, E. M., and Gruber, N.: Marine heatwaves under global warming, Nature, 560, 360–364,
550   https://doi.org/10.1038/s41586-018-0383-9, 2018.

551 Galbraith, P. S., Chassé, J., Shaw, J.-L., Dumas, J., and Bourassa, M.-N.: Physical oceanographic conditions in the Gulf of
552   St. Lawrence during 2023, Can. Tech. Rep. Hydrogr. Ocean Sci. 378 : v + 91 p, 2024.

553 Gonçalves Neto, A., Palter, J.B., Xu, X., Fratantoni, P. : Temporal Variability of the Labrador Current Pathways Around the
554   Tail of the Grand Banks at Intermediate Depths in a High-Resolution Ocean Circulation Model. J. Geophys. Res.
555   Oceans 128, e2022JC018756. https://doi.org/10.1029/2022JC018756, 2023.

556 Gregory, C. H., Artana, C., Lama, S., León-FonFay, D., Sala, J., Xiao, F., Xu, T., Capotondi, A., Martinez-Villalobos, C.,
557   and Holbrook, N. J.: Global Marine Heatwaves Under Different Flavors of ENSO, Geophysical Research Letters,
558   51, e2024GL110399, https://doi.org/10.1029/2024GL110399, 2024.

559 Hebert, D., Pettipas, R., Brickman, D., and Dever, M.: Meteorological, Sea Ice and Physical Oceanographic Conditions on
560   the Scotian Shelf and in the Gulf of Maine during 2012, DFO Can. Sci. Advis. Sec. Res. Doc. 2013/058. v + 46 p,
561   2013.

562 Hebert, D., Layton, C., Brickman, D., and Galbraith, P. S.: Physical Oceanographic Conditions on the Scotian Shelf and in
563   the Gulf of Maine during 2022, Can. Tech. Rep. Hydrogr. Ocean Sci. 359, vi + 81 p., 2023.

564 Hobday, A. J., Alexander, L. V., Perkins, S. E., Smale, D. A., Straub, S. C., Oliver, E. C. J., Benthuysen, J. A., Burrows, M.
565   T., Donat, M. G., Feng, M., Holbrook, N. J., Moore, P. J., Scannell, H. A., Sen Gupta, A., and Wernberg, T.: A
566   hierarchical approach to defining marine heatwaves, Progress in Oceanography, 141, 227–238,
567   https://doi.org/10.1016/j.pocean.2015.12.014, 2016.

568 Holbrook, N. J., Scannell, H. A., Sen Gupta, A., Benthuysen, J. A., Feng, M., Oliver, E. C. J., Alexander, L. V., Burrows, M.
569   T., Donat, M. G., Hobday, A. J., Moore, P. J., Perkins-Kirkpatrick, S. E., Smale, D. A., Straub, S. C., and
570   Wernberg, T.: A global assessment of marine heatwaves and their drivers, Nat Commun, 10, 2624,
571   https://doi.org/10.1038/s41467-019-10206-z, 2019.

572 Korus, J., Filgueira, R., and Grant, J.: Influence of temperature on the behaviour and physiology of Atlantic salmon (*Salmo*
573   *Salar*) on a commercial farm, Aquaculture, 589, 740978, https://doi.org/10.1016/j.aquaculture.2024.740978, 2024.

574 Lellouche, J.-M., Greiner, E., Bourdallé-Badie, R., Garric, G., Melet, A., Drévillon, M., Bricaud, C., Hamon, M., Le
575   Galloudec, O., Regnier, C., Candela, T., Testut, C.-E., Gasparin, F., Ruggiero, G., Benkiran, M., Drillet, Y., and Le
576   Traon, P.-Y.: The Copernicus Global 1/12° Oceanic and Sea Ice GLORYS12 Reanalysis, Front. Earth Sci., 9,
577   https://doi.org/10.3389/feart.2021.698876, 2021.

578 Loder, J.W., Petrie, B. and Gawarkiewicz, G.: The coastal ocean off northeastern North America: a large-scale view. Ch. 5
579   In: The Global Coastal Ocean: Regional Studies and Synthesis. The Sea, Vol. 11, A.R. Robinson and K.H. Brink
580   (eds.), John Wiley & Sons, Inc., p. 105-133, 1998.

581 Lu, Y., Wright, D. G., and Clarke, R. A.: Modelling deep seasonal temperature changes in the Labrador Sea, Geophysical
582   Research Letters, 33, https://doi.org/10.1029/2006GL027692, 2006.

583 Ma, Y., Lu, Y., Hu, X., Gilbert, D., Socolofsky, S. A., and Boufadel, M.: Model simulated freshwater transport along the
584   Labrador current east of the Grand Banks of Newfoundland, Front. Mar. Sci., 9,
585   https://doi.org/10.3389/fmars.2022.908306, 2022.

Meissner, T., Wentz, F. J., Scott, J., and Vazquez-Cuervo, J.: Sensitivity of Ocean Surface Salinity Measurements From Spaceborne L-Band Radiometers to Ancillary Sea Surface Temperature, IEEE Trans. Geosci. Remote Sensing, 54, 7105–7111, https://doi.org/10.1109/TGRS.2016.2596100, 2016.

Meyer-Gutbrod, E. L., Greene, C. H., Davies, K. T. A., and Johns, D. G.: Ocean Regime Shift is Driving Collapse of the North Atlantic Right Whale Population | Oceanography, 34(3):22–31, https://doi.org/10.5670/oceanog.2021.308, 2021..

Mills, K., Pershing, A., Brown, C., Chen, Y., Chiang, F.-S., Holland, D., Lehuta, S., Nye, J., Sun, J., Thomas, A., and Wahle, R.: Fisheries Management in a Changing Climate: Lessons From the 2012 Ocean Heat Wave in the Northwest Atlantic, oceanog, 26, https://doi.org/10.5670/oceanog.2013.27, 2013.

Mohamed, B., Barth, A., and Alvera-Azcárate, A.: Extreme marine heatwaves and cold-spells events in the Southern North Sea: classifications, patterns, and trends, Front. Mar. Sci., 10, https://doi.org/10.3389/fmars.2023.1258117, 2023.

Oliver, E. C. J., Donat, M. G., Burrows, M. T., Moore, P. J., Smale, D. A., Alexander, L. V., Benthuysen, J. A., Feng, M., Sen Gupta, A., Hobday, A. J., Holbrook, N. J., Perkins-Kirkpatrick, S. E., Scannell, H. A., Straub, S. C., and Wernberg, T.: Longer and more frequent marine heatwaves over the past century, Nat Commun, 9, 1324, https://doi.org/10.1038/s41467-018-03732-9, 2018.

Oliver, E. C. J., Benthuysen, J. A., Darmaraki, S., Donat, M. G., Hobday, A. J., Holbrook, N. J., Schlegel, R. W., and Sen Gupta, A.: Marine Heatwaves, Annual Review of Marine Science, 13, 313–342, https://doi.org/10.1146/annurev-marine-032720-095144, 2021.

Peal, R., Worsfold, M., and Good, S.: Comparing global trends in marine cold spells and marine heatwaves using reprocessed satellite data, State of the Planet, 1-osr7, 1–10, https://doi.org/10.5194/sp-1-osr7-3-2023, 2023.

Santora, J. A., Mantua, N. J., Schroeder, I. D., Field, J. C., Hazen, E. L., Bograd, S. J., Sydeman, W. J., Wells, B. K., Calambokidis, J., Saez, L., Lawson, D., and Forney, K. A.: Habitat compression and ecosystem shifts as potential links between marine heatwave and record whale entanglements, Nat Commun, 11, 536, https://doi.org/10.1038/s41467-019-14215-w, 2020.

Schlegel, R. W., Oliver, E. C. J., Wernberg, T., and Smit, A. J.: Nearshore and offshore co-occurrence of marine heatwaves and cold-spells, Progress in Oceanography, 151, 189–205, https://doi.org/10.1016/j.pocean.2017.01.004, 2017.

Schlegel, R. W., Oliver, E. C. J., and Chen, K.: Drivers of Marine Heatwaves in the Northwest Atlantic: The Role of Air–Sea Interaction During Onset and Decline, Front. Mar. Sci., 8, 627970, https://doi.org/10.3389/fmars.2021.627970, 2021a.

Schlegel, R. W., Darmaraki, S., Benthuysen, J. A., Filbee-Dexter, K., and Oliver, E. C. J.: Marine cold-spells, Progress in Oceanography, 198, 102684, https://doi.org/10.1016/j.pocean.2021.102684, 2021b.

Sen Gupta, A., Thomsen, M., Benthuysen, J. A., Hobday, A. J., Oliver, E., Alexander, L. V., Burrows, M. T., Donat, M. G., Feng, M., Holbrook, N. J., Perkins-Kirkpatrick, S., Moore, P. J., Rodrigues, R. R., Scannell, H. A., Taschetto, A. S., Ummenhofer, C. C., Wernberg, T., and Smale, D. A.: Drivers and impacts of the most extreme marine heatwave events, Sci Rep, 10, 19359, https://doi.org/10.1038/s41598-020-75445-3, 2020.

Shan, S. and Sheng, J.: Numerical Study of Topographic Effects on Wind-Driven Coastal Upwelling on the Scotian Shelf, Journal of Marine Science and Engineering, 10, 497, https://doi.org/10.3390/jmse10040497, 2022.

Smith, K. E., Sen Gupta, A., Amaya, D., Benthuysen, J. A., Burrows, M. T., Capotondi, A., Filbee-Dexter, K., Frölicher, T. L., Hobday, A. J., Holbrook, N. J., Malan, N., Moore, P. J., Oliver, E. C. J., Richaud, B., Salcedo-Castro, J., Smale, D. A., Thomsen, M., and Wernberg, T.: Baseline matters: Challenges and implications of different marine heatwave baselines, Progress in Oceanography, 231, 103404, https://doi.org/10.1016/j.pocean.2024.103404, 2025.

Soontiens, N., Andres, H. J., Coyne, J., Cyr, F., Galbraith, P. S., Penney, J.: An analysis of the 2023 summer and fall marine heat waves on the Newfoundland and Labrador Shelf: the impact of stratification, winds, and advection, Oceans State Report 9, 2025.

Thompson, K. R. and Demirov, E.: Skewness of sea level variability of the world's oceans, Journal of Geophysical Research: Oceans, 111, https://doi.org/10.1029/2004JC002839, 2006.

Umoh, J. U. and Thompson, K. R.: Surface heat flux, horizontal advection, and the seasonal evolution of water temperature on the Scotian Shelf, Journal of Geophysical Research: Oceans, 99, 20403–20416, https://doi.org/10.1029/94JC01620, 1994.

635 Wang, H., Lu, Y., Zhai, L., Chen, X., and Liu, S.: Variations of surface marine heatwaves in the Northwest Pacific during
636   1993–2019, Front. Mar. Sci., 11, 1323702, https://doi.org/10.3389/fmars.2024.1323702, 2024.

637 Wang, Y., Kajtar, J. B., Alexander, L. V., Pilo, G. S., and Holbrook, N. J.: Understanding the Changing Nature of Marine
638   Cold-Spells, Geophysical Research Letters, 49, e2021GL097002, https://doi.org/10.1029/2021GL097002, 2022.

639 Zhang, M., Cheng, Y., Wang, G., Shu, Q., Zhao, C., Zhang, Y., and Qiao, F.: Long-term ocean temperature trend and marine
640   heatwaves, J. Ocean. Limnol., https://doi.org/10.1007/s00343-023-3160-z, 2024.

641 Zhao, Z. and Marin, M.: A MATLAB toolbox to detect and analyze marine heatwaves, Journal of Open Source Software, 4,
642   1124, https://doi.org/10.21105/joss.01124, 2019.

643 Zisserson, B. and Cook, A.: Impact of bottom water temperature change on the southernmost snow crab fishery in the
644   Atlantic Ocean, Fisheries Research, 195, 12–18, https://doi.org/10.1016/j.fishres.2017.06.009, 2017.

645
646
647